# Thiol-Capping of CdTe Nanocrystals: An Alternative to Organometallic Synthetic Routes

**Nikolai Gaponik,* Dmitri V. Talapin, Andrey L. Rogach,* Kathrin Hoppe, Elena V. Shevchenko, Andreas Kornowski, Alexander Eychmüller, and Horst Weller**

*Institute of Physical Chemistry, University of Hamburg, Bundesstr. 45, 20146 Hamburg, Germany*

*Received: January 24, 2002; In Final Form: March 28, 2002*

New approaches to synthesize photostable thiol-capped CdTe nanocrystals are reported. Post-preparative size-selective precipitation and selective photochemical etching have been developed as methods providing an increase of photoluminescence quantum efficiency of the nanocrystals of up to 40%. Some advantages of thiol-capping in comparison to conventional organometallic syntheses of quantum dots are discussed.

## 1. Introduction

Semiconductor nanocrystals, or colloidal quantum dots (QDs), show unique size-dependent optical properties[1] and are currently of great interest for applications in optoelectronic[2−4] and photovoltaic[5,6] devices, optical amplifier media for telecommunication networks,[7,8] and for biolabeling.[9−12] The achievement of desired particle sizes over the largest possible range, narrow size distribution, good crystallinity, photostability, desired surface properties, and high luminescence quantum yields are the parameters that are considered to be characteristics of a "high quality" of the chemically prepared semiconductor QDs.

In the framework of the colloidal chemistry approach, high quality nanocrystals of different II−VI and III−V semiconductor materials can now be obtained. The two existent general strategies of nanocrystal preparations are an organometallic synthesis based on the high-temperature thermolysis of the precursors[13−19] or on a dehalosilylation reaction,[20,21] and the synthesis in an aqueous medium using polyphosphates[22] or thiols[23−27] as stabilizing agents. CdTe nanocrystals are the substance providing very high photoluminescence quantum efficiencies: the value of 65% at room temperature has been reported for organometallically prepared CdTe QDs.[17,28] However, potential applications of these nanocrystals are hindered due to an instability of their photoluminescence in air.[17,28] On the other hand, since the appearance of our first report on the aqueous synthesis of mercaptoethanol- and thioglycerol-capped CdTe nanocrystals in 1996,[24] sufficient progress has been made in the preparation and the design of the surface properties of thiol-capped CdTe nanocrystals whose luminescence is very stable and covers almost the whole visible spectral range (500−730 nm) depending on the particle size, as well as in their characterization[29,30] and their use for numerous applications. Worth mentioning is the utilization of luminescent thiol-capped CdTe QDs in light-emitting devices (LEDs),[4,31,32] photonic[33−36] and core−shell structures,[35,37,38] and as biological labels.[39] Recent investigations have shown the attractivity of this material for light energy conversion.[40] In this article we report on the aqueous synthesis (Section 3.1), the structure (Section 3.2), optical properties, and processability of thiol-capped CdTe nanocrystals, with an emphasis on the procedures leading to highly luminescent (room-temperature quantum efficiencies up to 40%) particles (Sections 3.3 and 3.4). We also discuss the advantages and disadvantages of different thiols used as capping agents of CdTe QDs which are relevant for the further design of surface properties of the nanocrystals, and stress some advantages of the aqueous synthesis in comparison to the organometallic routes, e.g., conventional TOPO-TOP (trioctylphosphine oxide−trioctylphosphine) approach (Section 3.5). Summarizing the experimental data available today, thiol-capped CdTe nanocrystals synthesized in aqueous solution represent a kind of stable highly luminescent core−shell QD system with a naturally sulfur-capped surface (CdS shell) created by mercapto-groups covalently attached to the surface cadmium atoms.

## 2. Experimental Section

All chemicals used were of analytical grade or of the highest purity available. $Al_2Te_3$ (lumps) used as a source of $H_2Te$ was purchased from CERAC Inc., WI. Milli-Q water (Millipore) was used as a solvent.

UV−vis absorption spectra were recorded with a Cary 50 spectrophotometer (Varian). Photoluminescence (PL) measurements were performed at room temperature using a FluoroMax-2 spectrofluorimeter (Instruments SA). The room-temperature PL quantum efficiency (QE) of CdTe nanocrystals was estimated following the procedure of ref 41 by comparison with Rhodamine 6G (laser grade, Lambda Physik) in ethanol (Uvasol) assuming its PL QE as 95%.[42] High-resolution transmission electron microscopy (HRTEM) and energy-dispersive X-ray analysis (EDX) were performed on a Philips CM-300 microscope operating at 300 kV. TEM samples were prepared by dropping diluted solutions of transferred in toluene (by surface exchange of capping agent with 1-dodecanethiol) CdTe nanocrystals onto 400-mesh carbon-coated copper grids with the excessive solvent immediately evaporated. Powder X-ray diffraction (XRD) measurements were carried out with a Philips X′Pert diffractometer (Cu Kα-radiation, variable entrance slit, Bragg−Brentano geometry, secondary monochromator). Samples for this study were prepared by placing finely dispersed powders of CdTe nanocrystals on standard Si supports.

To investigate the photostability of CdTe QDs, dilute colloidal solutions were irradiated for different time intervals with light of a 450 W xenon lamp cut around 400 nm by a band-pass filter having a bandwidth of ∼40 nm and a peak transmission of ∼40%.

* Corresponding authors. Fax: +49-40-428383452. E-mail addresses: gaponik@chemie.uni-hamburg.de. rogach@chemie.uni-hamburg.de.

10.1021/jp025541k CCC: $22.00 
Published on Web 06/21/2002

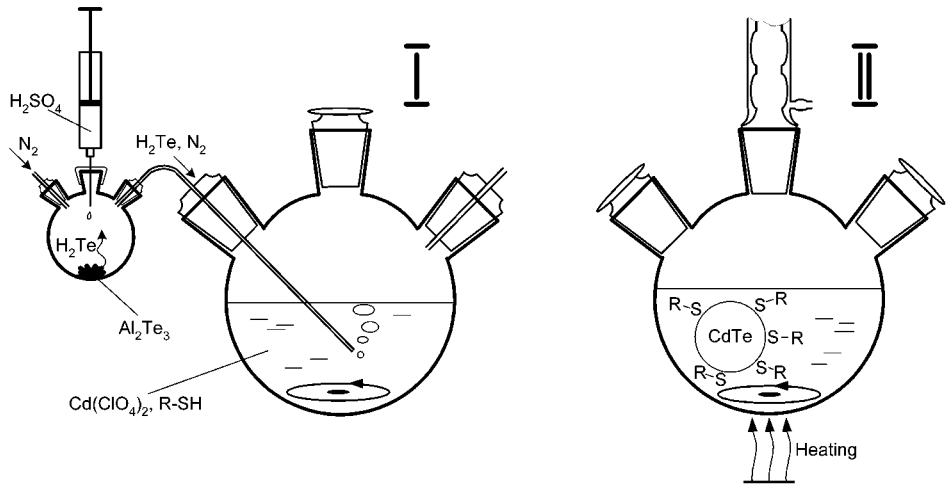


**Figure 1.** Schematic presentation of the synthesis of thiol-capped CdTe QDs. First stage: formation of CdTe precursors by introducing $H_2Te$ gas. Second stage: formation and growth of CdTe nanocrystals promoted by reflux.

**TABLE 1: Overview of the Conditions Used for the Aqueous Synthesis of CdTe Nanocrystals, Their Properties, and Additional Comments on Their Use**

| stabilizer | pH used for the synthesis | stability[a] of CdTe QDs | surface charge[b] of CdTe QDs | typical PL QE of as-prepared CdTe QDs | additional comments |
|---|---|---|---|---|---|
| 2-mercaptoethanol | 11.2−11.8 | stable | slightly negative in alkaline | <1% | "Magic" clusters of the (supposed) formula $Cd_{54}Te_{32}(SCH_2CH_2OH)_{32}^{8-}$ are formed[29] |
| 1-thioglycerol | 11.2−11.8 | stable | slightly negative in alkaline | 3% | Have been used for synthesis of highly luminescent CdHgTe QDs[27] and for electrophoretic deposition of closely packed films[43] |
| mixture (1:1) of 1-thioglycerol and 2,3-dimercapto-1-propanol | 11.2−11.8 | moderate | slightly negative in alkaline | 6% | High affinity to different surfaces (gold, glass, latex, polymers, etc.)[35,37] |
| thioglycolic acid (TGA) | 11.2−11.8 | stable | negative | 10% | Have been used for fabrication of LEDs and graded films by layer-by-layer assembly[4,44,45] and for electrophoretic deposition into pores of artificial opals.[36] Can potentially be used for bio-conjugation and for the synthesis of QDs conjugates. |
| 2-mercaptoethylamine (MA) | 5.6−5.9 | moderate | positive | 10% | Have been used for fabrication of latex core−semiconductor shell structures.[37] Can potentially be used for bio-conjugation and for the synthesis of QDs conjugates. |
| L-cysteine | 11.2−11.8 | moderate | negative or positive depending on the pH | 10% | Have been used for synthesis of conjugates with bovine serum albumin.[39] |
| 2-(dimethylamino)ethanethiol | 5.0−6.0 | moderate | positive | 30% | Under investigation. |

[a] "Stable" means here that colloidal solutions of CdTe QDs are stable for months and even years being stored under air in the dark at room temperature. "Moderate" means that colloidal solutions coagulate occasionally during the storage; however, they are generally stable for months as well. Independent of the stabilizer nature, CdTe QDs are generally stable (no oxidation, no or only very minor changes of the optical properties) for years in powder form and in closely packed or nanocrystal/polymer films being kept in the dark under air. [b] The charge of nanocrystals was evaluated from $\zeta$-potential measurements with employment of oppositely charged latex beads. The experimental conditions were chosen so that the $\zeta$-potential of the beads changed its sign after adsorption of a monolayer of nanoparticles.

## 3. Results and Discussion

**3.1. Synthesis of Thiol-Stabilized CdTe Nanocrystals.** In a typical synthesis (Figure 1) 0.985 g (2.35 mmol) of $Cd(ClO_4)_2 \cdot 6H_2O$ is dissolved in 125 mL of water, and 5.7 mmol of the thiol stabilizer (Table 1 shows mercapto-compounds typically used as capping agents) are added under stirring, followed by adjusting the pH to the appropriate values (depending on the stabilizer nature, see Table 1) by dropwise addition of 1 M solution of NaOH. Occasionally, the solution can remain slightly turbid at this stage because of the incomplete solubility of Cd thiolate complexes, but this does not influence the further synthesis. The solution is placed in a three-necked flask fitted with a septum and valves and is deaerated by $N_2$ bubbling for ~30 min. Under stirring, $H_2Te$ gas (generated by the reaction of 0.2 g (0.46 mmol) of $Al_2Te_3$ lumps with 15−20 mL of 0.5 M $H_2SO_4$ under $N_2$ atmosphere) is passed through the solution together with a slow nitrogen flow for ~20 min. CdTe precursors are formed at this stage which is accompanied by a change of the solution color, depending on the thiols used, to yellow (1-thioglycerol, 2-mercaptoethanol), orange (thioglycolic acid), or dark-red (2-(dimethylamino)ethanethiol, 2-mercaptoethylamine). They show an absorption spectrum being unstructured in the visible spectral region with a tail extending to 650−700 nm, and no luminescence. The precursors are converted to

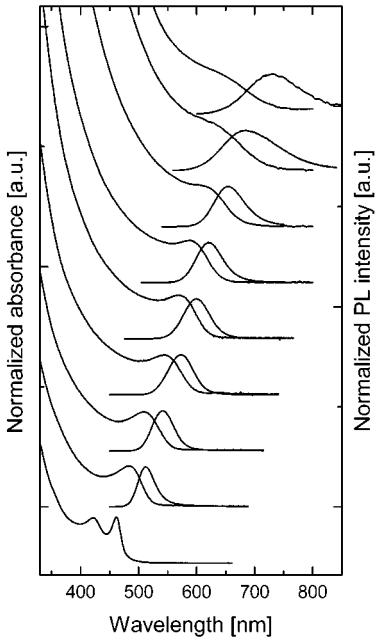


**Figure 2.** Absorption and PL spectra ($\lambda_{ex}$ = 400 nm) of CdTe nanocrystals taken as prepared. The stabilizers used were 2-mercaptoethanol, 2-(dimethylamino)ethanethiol, or thioglycolic acid. The smallest nanoparticles stabilized by 2-mercaptoethanol possess only a weak broad emission, associated with surface traps (not shown in the figure). Nanocrystals with emission maxima above 670 nm were obtained by additional injections of Cd and Te precursors.

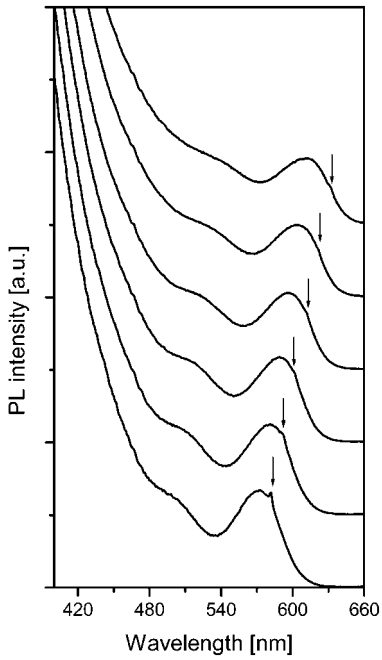


**Figure 3.** PL excitation spectra of TGA-capped CdTe nanocrystals showing well-resolved maxima of high-energy electronic transitions. The emission wavelengths are indicated by arrows.

CdTe nanocrystals by refluxing the reaction mixture at 100 °C under open-air conditions with condenser attached (Figure 1). A clearly resolved absorption maximum of the first electronic transition of CdTe QDs appears at ~420 nm in 5−10 min after beginning of reflux corresponding to the smallest CdTe nanocrystals (<2 nm size) which shifts to longer wavelengths as the particles grow in the course of heating. Green (luminescence maximum at ~510 nm) band-edge emission appears in 10−15 min after beginning of reflux when the CdTe nanocrystals reach the size of ~2 nm. The size of the CdTe QDs growing further is controlled by the duration of reflux and can easily be monitored by absorption and PL spectra. The duration of the heat treatment necessary to reach a certain particle size depends on the nature of the stabilizer. Thus, it takes 2−3 days to grow ~5 nm large CdTe nanocrystals (luminescence maximum at ~650 nm) in the presence of thioglycolic acid or mercaptoethylamine and up to 12 days when thioglycerol is used as a stabilizer. The same tendency was observed for the growth of CdSe nanocrystals stabilized with thio acids or thioalcohols.[25] To grow larger CdTe nanocrystals with the emission spreading into the near-IR (PL maximum up to 730 nm) additional injections of precursors are applied.

Note, that the synthesis of thiol-capped CdTe nanocrystals can also be done in a nonaqueous (dimethylformamide, DMF) solution by reaction of cadmium lactate with $H_2Te$ gas in the presence of thioglycerol as a stabilizer.[43] Because of the higher boiling point of DMF (130 °C) the particle growth proceeds much faster than in aqueous solution: it takes only 2 h to produce CdTe nanocrystals emitting at 650 nm. CdTe nanocrystals synthesized in DMF might be of special interest for forming composites with polymers soluble in organics.

Figure 2 shows typical absorption and room-temperature PL spectra of a size series of CdTe nanocrystals. The spectra were measured on as-prepared CdTe colloidal solutions which were taken from the refluxing reaction mixture at different intervals of time and diluted with water to provide the optical densities appropriate for PL measurements (about 0.1 at the excitation wavelength). All samples show a well-resolved absorption maximum of the first electronic transition indicating a sufficiently narrow size distribution of the CdTe QDs, which shifts to the longer wavelengths with increasing size of the nanocrystals as a consequence of the quantum confinement. The room-temperature PL excitation spectra (Figure 3) also display electronic transitions at higher energies. PLE technique allows detection of the luminescence emitted by particles with selected size. The difference between PLE and absorption spectra is a result of the inhomogeneous broadening which affects the UV−vis spectra to a greater degree than PLE ones. The PL bands (Figure 2) are located close to the absorption thresholds (so-called band-edge or "excitonic" photoluminescence) and are sufficiently narrow (full width at half-maximum, fwhm, as low as 35 nm being increased up to 55−60 nm for size fractions of large CdTe nanocrystals). The position of the PL maximum of the smallest (~2 nm) luminescing CdTe QDs is located at 510 nm (green emission), whereas the largest (~6 nm) CdTe nanocrystals obtained emit in the near-IR with a PL maximum at 730 nm. The whole spectral range between these two wavelengths is covered by the intermediate sizes of CdTe QDs. The PL QE of as-synthesized CdTe nanocrystals depends on the nature of the stabilizing agent (Table 1) and lies typically between 3 and 10%, although values of 30−35% for 2-(dimethylamino)ethanethiol-stabilized nanocrystals were attained. In most cases it can be sufficiently improved by post-preparative treatments of the nanocrystals as will be shown below.

Table 1 provides an overview of different thiols used by us as capping agents for CdTe nanocrystals. As already mentioned above, the nature of the thiol influences the particle growth and the PL QE of as-synthesized CdTe nanocrystals. Besides that, each type of stabilizer has its own advantages and disadvantages allowing the use of CdTe nanocrystals capped by varying thiols for different purposes. This is also briefly summarized in Table 1. CdTe QDs stabilized by thioglycolic acid (TGA) or by mercaptoethylamine (MA) show efficient luminescence as prepared and possess either negative or positive surface charge because of the surface carboxylic or amino groups, respectively.

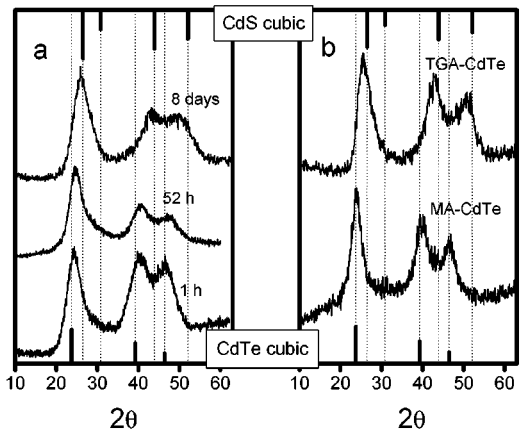


**Figure 4.** Temporal evolution of powder X-ray diffractograms during the synthesis of thioglycerol-capped CdTe nanocrystals (a). X-ray diffractograms of CdTe nanocrystals obtained in aqueous solutions in the presence of TGA and MA (b).

The possibility to manipulate these nanocrystals, e.g., by the layer-by-layer technique[4,44,45] or by electrophoresis,[36,43,45] and to use the free functional groups of the capping molecules for conjugation[39] makes them especially attractive for fabrication of functional materials. In the following sections, we mainly discuss the TGA- and MA-capped CdTe nanocrystals and describe ways of further improvement of their photoluminescence efficiency.

**3.2. Structural Characterization of Thiol-Capped CdTe Nanocrystals.** Figure 4 shows XRD patterns obtained from powdered precipitated fractions of CdTe nanocrystals synthesized at different conditions. The nanocrystals belong to the cubic (zinc blende) structure which is also the dominant crystal phase of bulk CdTe. However, the positions of the XRD reflexes of CdTe QDs synthesized under prolonged refluxing in the presence of thioglycolic acid or thioglycerol (Figure 4) are intermediate between the values of the cubic CdTe and the cubic CdS phases. As discussed in ref 43, prolonged refluxing of the aqueous colloidal solutions of CdTe nanocrystals in the presence of an excess of thiols in basic media leads to partial hydrolysis of the thiols and to the incorporation of the sulfur from the thiol molecules into the growing nanoparticles. Mixed CdTe(S) QDs, most probably with some gradient of sulfur distribution from inside the nanocrystals to the surface, are formed under these conditions as evidenced from the temporal evolution of the XRD patterns during refluxing (Figure 4a). Indeed, the smaller nanocrystals synthesized at moderate conditions (short refluxing time) show only slight deviations of the XRD reflexes from CdTe zinc blende diffraction patterns. The use of DMF instead of water as a solvent allows the prevention of the hydrolysis of thiols and, thus, diminishes the incorporation of sulfur into largely grown nanocrystals.[43] The aqueous synthesis performed at comparatively low pH values (5.6−5.9) in the presence of 2-mercaptoethylamine as a stabilizer leads to the formation of CdTe nanocrystals whose XRD patterns show only slight traces of a CdS phase (Figure 4b).

HRTEM investigations of CdTe nanocrystals grown at different conditions confirmed the XRD data. The longer the time of refluxing in the basic medium, the larger was the sulfur content in the mixed CdTe(S) nanocrystals as indicated by the lattice plane distances in the HRTEM images being intermediate between cubic CdTe and cubic CdS phases.[43] In contrast, MA-capped CdTe nanocrystals synthesized at slightly acidic pH showed the lattice plane distances of the cubic CdTe phase. As is evident from Figure 5 the thiol-capped CdTe nanoparticles

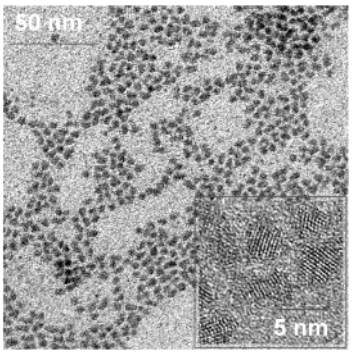


**Figure 5.** TEM overview and HRTEM (inset) images of TGA-capped CdTe nanocrystals. The particles were transferred from water to toluene in the presence of 1-dodecanethiol in order to achieve their better separation on the TEM grids.

are crystalline, sufficiently monodisperse and well separated, with a mean size of ∼4.5 nm which is in good accordance with the size calculated from the XRD data by the Scherrer equation.

Thus, both XRD and TEM investigations show that crystalline (cubic zinc blende structure) particles of either pure CdTe or mixed CdTe(S) phase are formed in the aqueous synthesis depending on the reaction conditions (pH value, duration of reflux, nature of stabilizer).

Worth mentioning is the temperature-dependent EXAFS study carried out on 2-mercaptoethanol capped CdTe nanocrystals and reported in detail in ref 29. The investigation allowed the separation of the structural and dynamic properties of the CdTe core and the Cd-SR shell. The formula $[Cd_{54}Te_{32}(SCH_2CH_2OH)_{52}]^{8-}$ was suggested for these extremely small clusters consisting of a tetrahedral CdTe zinc blende core partially coated by a Cd−SR surface layer.

**3.3. Photostability of Thiol-Capped CdTe Nanocrystals.** As indicated in Table 1, colloidal solutions of CdTe QDs are stable and do not change their optical properties for months and even years (depending on the nature of the stabilizer) being kept under air in the dark at room temperature. Light sensitivity (photochemical stability) of aqueous CdTe colloids was found to be strongly dependent on the presence of oxygen and free stabilizer molecules in solution and can be greatly improved by keeping them under inert atmosphere. We have compared the room-temperature photostability of aqueous colloids of TGA-capped and MA-capped CdTe nanocrystals with the photostability of organometallically synthesized CdTe QDs and TOPO-capped CdSe nanocrystals. The latter QDs were reported to be stable enough for, e.g., applications in light-emitting devices.[3,46]

The optical densities of irradiated solutions of TGA-capped CdTe QDs in water and TOPO-capped CdSe QDs in toluene were 0.15 at 400 nm. The absorption and the PL spectra of CdTe and CdSe nanocrystals were checked after different intervals of irradiation time. The long-term photostability of deaerated solutions of the both materials was found to be comparable and very high. The photodegradation of TGA-capped CdTe QDs in oxygen-saturated solutions proceeded approximately 20 times faster than under airless conditions. However, taking into account the rigid conditions of illumination their photostability even in this case was very high in comparison with organometallically synthesized CdTe QDs[17] and was comparable with the stability of TOPO-capped CdSe nanocrystals (Figure 6).

The mechanism of nanocrystal photodegradation seems to be different in the cases of TGA-capped CdTe and TOPO-capped CdSe nanocrystals. Both in airless and in oxygen-

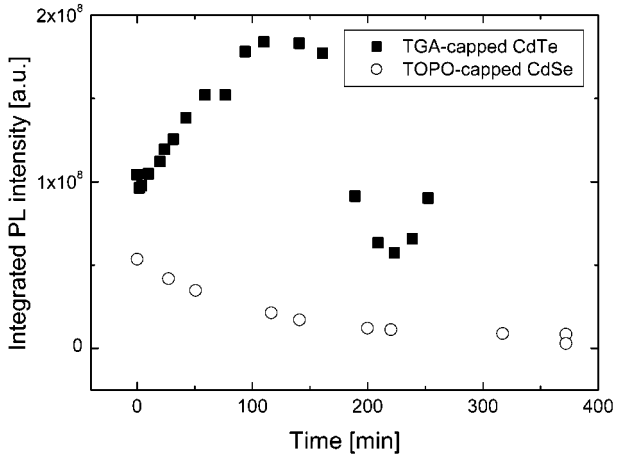


**Figure 6.** Evolution of the relative quantum efficiency of photoluminescence of oxygen-saturated solutions of TGA-capped CdTe and TOPO-capped CdSe QDs under irradiation with 400 nm light of a 450 W xenon lamp.

saturated solutions the illumination of CdTe nanocrystals leads first to a sufficient improvement of their PL QE, followed by a gradual quenching of PL intensity and finally to coagulation of the colloid. The nanocrystals in the precipitate normally still luminesce. In the case of TOPO-capped CdSe nanocrystals the PL QE slowly goes down during the illumination until the luminescence disappeared completely, while no coagulation is observed (Figure 6).

The photostability of MA-capped CdTe nanocrystals in aerated aqueous solutions was found to be lower compared to that of the TGA-capped CdTe QDs and no improvement of the PL QE was observed at initial stages of irradiation. The difference between the behavior of TGA- and MA-stabilized CdTe QDs originates most probably from their structural difference. The TGA-capped nanocrystals are essentially in the mixed CdTe(S) phase with sulfur-enriched pre-surface layers, whereas MA-capped particles are almost pure CdTe. The irradiation promotes oxidation of unsaturated Te atoms which were recently identified as hole traps by optically detected magnetic resonance[47] and are known to be highly susceptible to oxidation.[48] This treatment leads to an improvement of the CdS shell around the CdTe core via substitution of oxidized surface Te sites by sulfur from the stabilizer molecules. The formation of such a shell enhances the PL efficiency of TGA-capped CdTe QDs at the initial stages of illumination and greatly inhibits the following photodegradation of the nanocrystals. In fact, an enhancement of the PL efficiency at initial stages of irradiation was also observed for CdSe/ZnS core−shell nanocrystals.[49] In the case of MA-stabilized CdTe QDs where sulfur atoms are hardly present in the crystalline structure, a complete outer CdS shell cannot be formed at the expense of thiol molecules of the stabilizing shell resulting in their faster photodegradation. The absence of a stabilizing CdS shell in the case of organometallically synthesized CdTe nanocrystals whose surface is capped by TOP and amines[17] causes a very quick loss of the photoluminescence in air as well.

In addition to the above-mentioned processes, a photocatalytic oxidation of thiol molecules on the surface of nanocrystals can also take place as was shown for thiol-capped CdSe nanocrystals.[50] The thiol ligands on the surface of the QDs convert into disulfides under irradiation leading to precipitation of the nanocrystals if no new thiol ligands are available in solution. This model correlates well with the behavior of the TGA-capped CdTe nanocrystals allowing the explanation of their higher photostability in the presence of the excess of free thiol stabilizer in solution.[51]

The photostability of all kinds of thiol-capped CdTe nanocrystals in the solid state (powders, closely packed QD films, nanocrystal/polymer composites) is comparable, very high, and independent of the nature of the stabilizer. Thus, a month of storage under daylight and air did not cause recognizable changes of the optical properties of spin-coated or casted closely packed films of both TGA- and MA-stabilized nanocrystals. The layer-by-layer formed films of TGA-capped CdTe QDs with poly(diallyldimethylammonium chloride) as a polyelectrolyte also remained highly luminescent under the same conditions, but a slight bleaching was observed within weeks.

**3.4. Post-Preparative Improvement of the Photoluminescence Efficiency of Thiol-Capped CdTe Nanocrystals.** Taking into account the growing demand on strongly luminescing semiconductor nanocrystals for light-emitting devices[2−4,46] and tagging applications,[9−12] several strategies of improvement of the PL efficiency of thiol-capped CdTe nanocrystals have been developed. The earliest attempt was the study of the pH dependence on the luminescence efficiency of TGA-capped CdTe QDs.[51] It was found that the PL QE can be enhanced up to 5 times (from 3−4% being characteristic for the TGA-capped CdTe QDs synthesized by using a NaHTe solution as the tellurium source to 18−20%) by decreasing the pH of the colloidal solution to 4.5−5.0 in the presence of excessive thioglycolic acid. At these conditions, a shell of thiolate complexes is probably formed at the surface of the CdTe nanocrystals acting as a wide-bandgap material analogous to, for example, a CdS[52] or ZnS shell[16,53] on CdSe cores and eliminating the surface traps which are centers of nonradiative recombination.

Further studies have shown the possibility of a sufficiently larger improvement of the PL efficiency (up to 40% at room temperature) of thiol-capped CdTe nanocrystals. Importantly, simple methods of the post-preparative size-selective precipitation and selective photochemical etching have been found to work well, yielding highly luminescent CdTe nanocrystal fractions. Both methods are discussed below in more detail.

*3.4.1. Size-Selective Precipitation.* The post-preparative size-selective precipitation procedure[13,54] can successfully be applied for isolation of thiol-capped CdTe nanocrystals from their crude solutions and for narrowing down their size distribution. The method is based on the gradual precipitation of the nanocrystals induced by addition of a nonsolvent (the largest particles precipitate first) allowing the separation of the initial colloidal solution into several fractions of nanocrystals with narrowed size distributions. In the case of thiol-capped CdTe nanocrystals, the procedure is carried out under air and is typically as follows. A portion of as-prepared colloidal solution containing CdTe nanocrystals of a certain mean size is concentrated ∼5 times using a rotary evaporator. Then, 2-propanol is added dropwise under stirring until the solution becomes slightly turbid. The turbid dispersion is left stirring for further 15 min, and the precipitate containing the first fraction of CdTe nanocrystals is isolated from the supernatant by centrifugation. Another portion of 2-propanol is added dropwise to the supernatant to obtain the second precipitated fraction of CdTe nanocrystals and so on. This procedure can be repeated several times to obtain up to 10−12 size-selected fractions of CdTe nanocrystals from the initial solution. The precipitated nanocrystal fractions can be redissolved in water or dried and kept during a long period of time as water-soluble powders.

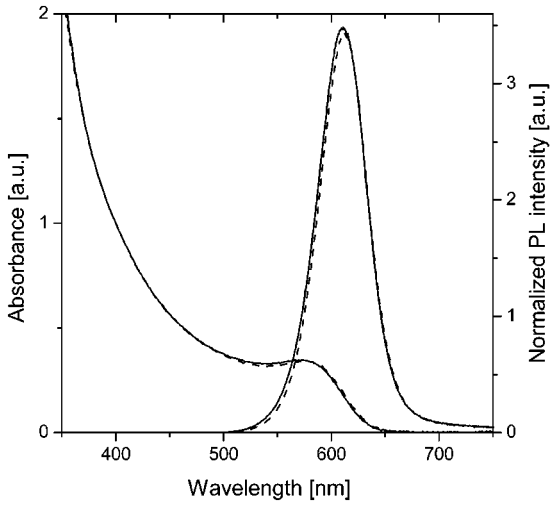


**Figure 7.** Absorption and PL spectra of an as-prepared crude solution of CdTe nanocrystals (solid line) and of a solution obtained by re-mixing all size-selected fractions isolated from this crude solution (dashed line).

Importantly, no changes in the optical properties of the thiol-capped CdTe nanocrystals are induced by their size-selective precipitation. Thus, a comparison of the initial crude solution of TGA-capped CdTe QDs with a solution prepared by mixing all size-selectively isolated fractions in the same proportions as they were presented in the crude solution shows nearly quantitative agreement between their UV−vis and PL spectra (Figure 7). This is probably a result of the strong capping of CdTe nanocrystals with thiol molecules during the post-preparative treatment. In contrast, in the case of organometallically synthesized CdSe or InAs nanocrystals a systematic decrease of the PL QE of size-selected fractions in comparison with their initial crude solutions was observed due to the partial removal of the more labile TOPO-stabilizing shells under conditions when the concentration of the excessive TOP in the solution was low.[55]

Figure 8 shows absorption and PL spectra of the size-selected fractions obtained from two different portions of TGA-capped CdTe nanocrystals. The portions were taken from the same crude solution of the grown nanoparticles after different refluxing times, and thus contained CdTe nanocrystals of different mean sizes. The particle size distribution in each size-selected fraction is, as expected, narrower than in the initial crude solution leading to a better pronounced electronic transition in the absorption spectra and to narrower PL bands (fwhm 38−52 nm, in initial solutions ∼46−56 nm).

There is a clear dependence of the efficiency of the band-edge PL on the "fraction number" of CdTe nanocrystals (Figure 8). The increase of the PL intensity is nonmonotonic: the maximum of the PL efficiency is always achieved for a fraction lying in the middle of the size-selected series, independent of

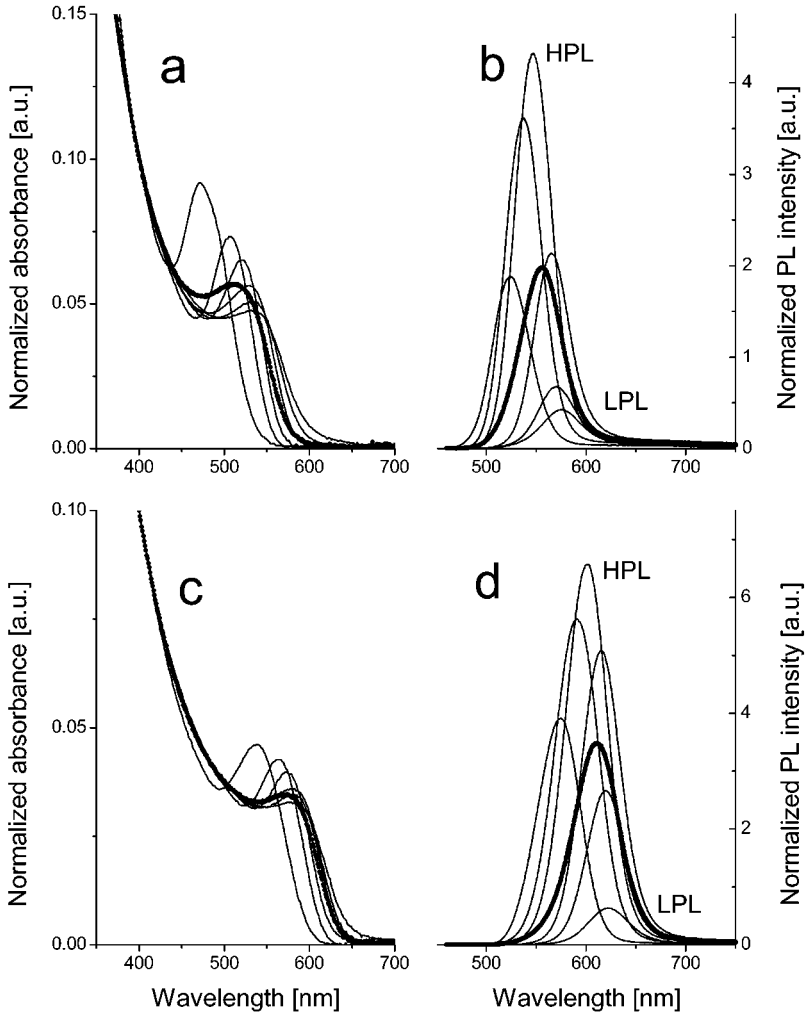


**Figure 8.** Absorption (a, c) and PL (b, d) spectra of size-selected fractions isolated from two portions of a crude solution of CdTe nanocrystals taken after refluxing for 2.5 h (a, b,) and 30 h (c, d), respectively. The absorption and PL spectra of as-prepared crude solutions (bold lines) are added for comparison. PL intensities are normalized to identical absorbance at the excitation wavelength (400 nm).

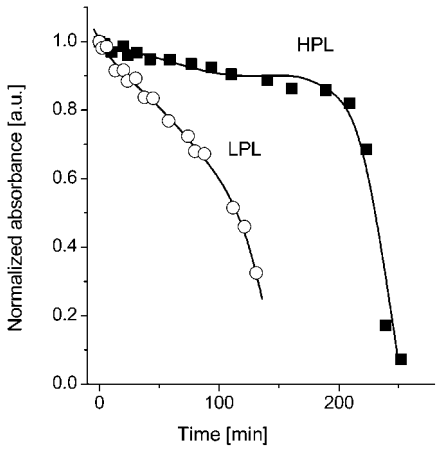


**Figure 9.** The temporal evolution of the absorbance at 400 nm of the LPL (○) and the HPL (■) fractions of CdTe nanocrystals under irradiation with 400 nm light of a 450 W xenon lamp in oxygen-saturated solutions. The absorbance is normalized to the initial value (i.e., before irradiation).

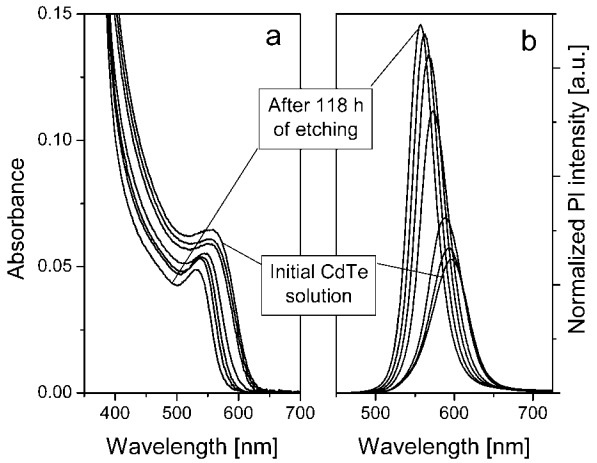


**Figure 10.** Evolution of absorption (left) and PL (right) spectra of TGA-stabilized CdTe nanocrystals exposed to selective etching at the low energy side of the absorption spectrum. The PL spectra are normalized to the absorption at the excitation wavelength (450 nm).

the mean particle size of the nanocrystals in the initial crude solution. The difference between the intensities of the fractions of CdTe QDs with the lowest and the highest PL efficiency (referred in Figures 8 and 9 as LPL and HPL fractions, respectively) reaches about an order of magnitude, with a PL QE of 25−30% for the HPL fractions. In addition, the photostability of the HPL fractions is higher than the photostability of any other fraction obtained from the same portion of the crude solution (Figure 9).

The possibility to divide any crude solution into fractions of nanocrystals differing in their photoluminescence intensity and photostability was found by us for TOPO-capped CdSe and TOP-capped InAs QDs as well,[55] which indicates a general character of this phenomenon for any ensemble of colloidal semiconductor nanocrystals. The nonmonotonic distribution of PL intensities within the ensembles of QDs is inherent to the particle growth via an Ostwald ripening mechanism and originates, most probably, from different degrees of the nanocrystal surface disorder. Detailed investigation of this phenomenon is presented elsewhere.[55]

Thus, highly luminescent fractions of thiol-capped CdTe nanocrystals with PL QE of 20−30% are present in any portion of the crude solution and can be easily extracted by the size-selective precipitation technique. Furthermore, the PL efficiency of the HPL fractions of TGA-capped CdTe nanocrystals can be further enhanced up to 40% by the formation of a shell of cadmium thiolate complexes at the surface of the nanoparticles using the method of ref 51.

*3.4.2. Selective Photochemical Etching.* As mentioned in Section 3.3, the photoluminescence efficiency of TGA-capped CdTe nanocrystals increases at the initial stages of photooxidation, presumably due to the etching of tellurium trap states and an improvement of the CdS shell. Further investigations of photochemical etching showed the possibility of using this technique to enhance the luminescence of CdTe nanocrystals. The etching was carried out by illumination with a 450 W xenon lamp under aerobic conditions. The high-energy part of the lamp spectrum was cut off by optical filters in order to illuminate the samples near the absorption edges. Under these conditions an exposure for 5 days typically leads to both a ∼3-fold improvement of the PL QE (up to 30%) and narrowing the PL band of the crude solutions of TGA-stabilized CdTe QDs (Figure 10). Surprisingly, the positions of the PL maxima of the highly luminescent fractions obtained by photochemical etching coincide almost exactly (±1 nm) with those of the size-selectively precipitated HPL fractions when the same crude solutions are taken. The photochemical etching under polychromatic light leads to an increase of the PL QE up to 40% coming along with a broadening of the photoluminescence and absorption bands owing to different rates of etching of different nanocrystals in the ensemble. We suggest that the improvement of the PL QE is due to the eliminating of defect states (or carrier traps)—most probably unsaturated surface tellurium atoms.[47] The nanocrystals possessing the most defect states dissolve primarily during photochemical etching. On the other hand the elimination of a few (or single) Te traps does not lead to the degradation of the low-defect QDs due to the passivating role of their CdS shell. Moreover, the vacancies formed can be successfully saturated by an excess of thiol molecules being available in solution.

The fractions of etched CdTe nanocrystals with PL QE of ∼40% show a temporal stability against coagulation comparable with the initial solutions of the nanocrystals. The luminescence properties of the former as solid films (both casted and spin-coated) were found to be stable for at least 4 weeks under daylight conditions.

**3.5. Aqueous Synthesis vs Organometallic Approach: Advantages and Disadvantages.** In this section we discuss some general advantages of the aqueous synthesis and compare some characteristics of thiol-capped CdTe nanocrystals with corresponding data of organometallically synthesized QDs. The comparison with organometallically synthesized QDs will be done based both on their properties published in the literature and on our own experiences in the synthesis and handling of CdTe,[17] CdSe,[16,55,56] InP,[57] InAs,[55] and CdSe/ZnS[16] nanocrystals.

Among the advantages of the aqueous synthesis its simplicity and high reproducibility should be mentioned. Thus, colloids of CdTe nanocrystals with a particle size distribution about 10% can be prepared without the hot-injection technique which is necessary for the synthesis of nanocrystals in TOPO-TOP mixture (e.g., CdSe,[13] CdTe,[28] InAs[58]). As a result, the aqueous synthesis of thiol-capped nanocrystals can be carried out equally effectively on a vast scale, whereas the scaling up of the organometallic synthesis is difficult[59] due to its poor reproducibility[15,18] and the use of extremely dangerous reactants (e.g., dimethylcadmium). The aqueous synthesis was successfully carried out by us yielding up to 10 g of CdTe nanocrystals per synthesis and further scaling up is possible. These nanocrystals

can be precipitated, washed and kept in the dry state under ambient conditions as long as two years being stable and resoluble in water.

Keeping in mind the potential importance of highly luminescent nanocrystals for large-scale applications, we also estimated the cost of equimolar amounts (with respect to formula unit, i.e., CdTe and CdSe) of TGA-capped CdTe and TOPO-capped CdSe nanocrystals whose luminescence efficiencies and photostabilities are similar. The costs of chemicals were compared using Aldrich'2001 prices for most of the chemicals, Strem'2001 price for dimethylcadmium and CERAC Inc.'2001 price for $Al_2Te_3$. The synthesis of CdSe QDs is about 8 times more expensive. In the case of organometallically prepared core/shell nanocrystals (e.g., CdSe/ZnS and CdSe/CdS) this difference reaches orders of magnitude. However, in recent papers by Peng et al. low cost and less hazardous precursors (CdO, cadmium acetate, etc.) and stabilizing mixtures based on fatty acids were applied for the synthesis of nonaqueous highly luminescent CdSe nanocrystals.[18,19] The use of these alternative synthetic routes might considerably decrease the cost of organometallically prepared luminescent QDs.

Nanocrystals synthesized by the aqueous approach do not possess the degree of crystallinity of the organometallically prepared QDs, where high annealing temperatures (200−360 °C) are used during the synthesis. A very effective separation of nucleation and growth stages achieved in the organometallic synthesis by the so-called hot-injection technique[13] allows to reach narrower size distributions of the nanocrystals in comparison with those prepared in aqueous solutions. However, the aqueous approach generally allows the synthesis of smaller QDs, both CdTe and CdSe,[25] and the post-preparative size-selective precipitation procedure works more reproducible in the case of aqueous colloids in terms of retaining the luminescence properties, as discussed in Section 3.4.1.

The possibility of controlling the surface charge and other surface properties of thiol-capped QDs simply by the choice of the stabilizing mercapto-compound with appropriate free functional groups is definitely important, especially when water-soluble nanocrystals are needed, e.g., for fluorescent tagging applications. We refer the reader to the paper[12] for the criticism on the reported routes to make TOPO-capped nanocrystals with CdSe cores water-soluble, pointing out that the stepwise procedure proposed in this paper yielded CdSe/ZnS core−shell QDs whose PL QE does not exceed 10−20%. TGA-capped water-soluble CdTe nanocrystals with stable PL QE up to 40% reported in the present study might be an useful alternative in this case.

## 4. Conclusions

Thiol-capped CdTe nanocrystals represent a kind of core−shell system with a naturally sulfur-capped surface (CdS shell) created by mercapto-groups covalently attached to the surface cadmium atoms. By reaction conditions facilitating the formation of mixed CdTe(S) nanocrystals, as mentioned above for the TGA-capped CdTe QDs, the sulfur-rich region is most probably stretched from the surface into the nanocrystal. Importantly, the synthesis of such kind of core−shell nanocrystals naturally occurs in one step, as the sulfur originates from the stabilizing thiol molecules during the particle growth. At the bulk CdTe/CdS interface, the conduction band step, i.e., the offset of the absolute band position, is close to zero, whereas the valence band step is ∼1 eV as given in ref 60. The wave functions calculated for a CdTe/CdS system with the particle-in-a-box model[61] show a delocalization of the electron through the entire structure and the confinement of the hole in the CdTe core—the same picture as reported for the CdSe/CdS nanocrystals providing the photostability and electronic accessibility.[52] The effective screening of the hole by the shell explains the high photostability of these nanocrystals, since the main photodegradation mechanism is the photooxidation of surface tellurium atoms requiring oxygen and holes.[22,48] The weak localization of electrons promotes the electronic accessibility of thiol-capped CdTe nanocrystals, allowing, e.g., an effective electron injection important for LED applications.[4,31,32] The additional functional groups of the thiol capping molecules of the nanocrystals provides their water solubility, high processability, and surface charge desired.

**Acknowledgment.** We thank J. Kolny for assistance with powder X-ray diffraction measurements, and Prof. Dr. M. Gao for useful discussions. This work was supported in part by the DFG Schwerpunktprogramm "Photonic Crystals", the BMBF-Philips research project, NATO Collaborative Linkage Grant CLG 976365 and Fond der Chemischen Industrie.

## References and Notes

(1) Gaponenko, S. V. *Optical Properties of Semiconductor Nanocrystals*; Cambridge University Press: Cambridge, 1998.
(2) Schlamp, M. C.; Peng, X.; Alivisatos, A. P. *J. Appl. Phys.* **1997**, *82*, 5837.
(3) Mattoussi, H.; Radzilowski, L. H.; Dabbousi, B. O.; Thomas, E. L.; Bawendi, M. G.; Rubner, M. F. *J. Appl. Phys.* **1998**, *83*, 7965.
(4) Gao, M.; Lesser, C.; Kirstein, S.; Möhwald, H.; Rogach, A. L.; Weller, H. *J. Appl. Phys.* **2000**, 87, 2297.
(5) Greenham, N. C.; Peng, X.; Alivisatos, A. P. *Phys. Rev. B* **1996**, *54*, 17628.
(6) Barnham, K.; Marques, J. L.; Hassard, J.; O'Brien, P. *Appl. Phys. Lett.* **2000**, *76*, 1197.
(7) Harrison, M. T.; Kershaw, S. V.; Burt, M. G.; Rogach, A. L.; Kornowski, A.; Eychmüller, A.; Weller, H. *Pure Appl. Chem.* **2000**, *72*, 295.
(8) Kershaw, S. V.; Harrison, M. T.; Rogach, A. L.; Kornowski, A. *IEEE J. Select. Topics Quantum Electron.* **2000**, *6*, 534.
(9) Bruchez, M. P.; Moronne, M.; Gin, P.; Weiss, S.; Alivisatos, A. P. *Science* **1998**, *281*, 2013.
(10) Chan, W. C. W.; Nie, S. *Science* **1998**, *281*, 2016.
(11) Han, M.; Gao, X.; Su, J. Z.; Nie, S. *Nature Biotechnol.* **2001**, *19*, 631.
(12) Mattoussi, H.; Mauro, J. M.; Goldman, E. R.; Anderson, G. P.; Sundar, V. C.; Mikulec, F. V.; Bawendi, M. G. *J. Am. Chem. Soc.* **2000**, *122*, 12142.
(13) Murray, C. B.; Norris, D. J.; Bawendi, M. G. *J. Am. Chem. Soc.* **1993**, *115*, 8706.
(14) Katari, J. E. B.; Colvin, V.; Alivisatos, A. P. *J. Phys. Chem.* **1994**, *98*, 4109.
(15) Peng, Z. A.; Peng, X. *J. Am. Chem. Soc.* **2001**, *123*, 183.
(16) Talapin, D. V.; Rogach, A. L.; Kornowski, A.; Haase, M.; Weller, H. *Nano Lett.* **2001**, *1*, 207.
(17) Talapin, D. V.; Haubold, S.; Rogach, A. L.; Kornowski, A.; Haase, M.; Weller, H. *J. Phys. Chem. B* **2001**, *105*, 2260.
(18) Qu, L.; Peng, Z. A.; Peng, X. *Nano Lett.* **2001**, *1*, 333.
(19) Qu, L.; Peng, X. *J. Am. Chem. Soc.* **2002**, *124*, 2049.
(20) Micic, O. I.; Curtis, C. J.; Jones, K. M.; Sprague, J. R.; Nozik, A. J. *J. Phys. Chem.* **1994**, *98*, 4966.
(21) Cao, Y. W.; Banin, U. *J. Am. Chem. Soc.* **2000**, *122*, 9692.
(22) Spanhel, L.; Haase, M.; Weller, H.; Henglein, A. *J. Am. Chem. Soc.* **1987**, *109*, 5649.
(23) Vossmeyer, T.; Katsikas, L.; Giersig, M.; Popovic, I. G.; Diesner, K.; Chemseddine, A.; Eychmüller, A.; Weller, H. *J. Phys. Chem.* **1994**, *98*, 7665.
(24) Rogach, A. L.; Katsikas, L.; Kornowski, A.; Su, D.; Eychmüller, A.; Weller, H. *Ber. Bunsen-Ges. Phys. Chem.* **1996**, *100*, 1772.
(25) Rogach, A. L.; Kornowski, A.; Gao, M.; Eychmüller, A.; Weller, H. *J. Phys. Chem. B* **1999**, *103*, 3065.
(26) Rogach, A. L.;, Kershaw, S. V.; Burt, M. G.; Harrison, M.; Kornowski, A.; Eychmüller, A.; Weller, H. *Adv. Mater.* **1999**, *11*, 552.
(27) Harrison, M. T.; Kershaw, S. V.; Burt, M. G.; Eychmüller, A.; Weller, H.; Rogach, A. L. *Mater. Sci. Eng. B* **2000**, *69*, 355.
(28) Mikulec, F. V.; Bawendi, M. G.; Kim, S. Patent WO 01/07689.

(29) Rockenberger, J.; Tröger, L.; Rogach, A. L.; Tischer, M.; Grundmann, M.; Eychmüller, A.; Weller, H. *J. Chem. Phys.* **1998**, *108*, 7807.
(30) Kapitonov, A. M.; Stupak, A. P.; Gaponenko, S. V.; Petrov, E. P.; Rogach, A. L.; Eychmüller, A. *J. Phys. Chem. B* **1999**, *103*, 10109.
(31) Gaponik, N. P.; Talapin, D. V.; Rogach, A. L. *Phys. Chem. Chem. Phys.* **1999**, *1*, 1787.
(32) Gaponik, N. P.; Talapin, D. V.; Rogach, A. L.; Eychmüller, A. *J. Mater. Chem.* **2000**, *10*, 2163.
(33) Gaponenko, S. V.; Kapitonov, A. M.; Bogomolov, V. N.; Prokofiev, A. V.; Eychmüller, A.; Rogach, A. L. *JETP Lett.* **1998**, *68*, 142.
(34) Gaponenko, S. V.; Bogomolov, V. N.; Petrov, E. P.; Kapitonov, A. M.; Yarotsky, D. A.; Kalosha, I. I.; Eychmüller, A.; Rogach, A. L.; McGilp, J.; Woggon, U.; Gindele, F. *IEEE J. Lightwave Technol.* **1999**, *17*, 2128.
(35) Rogach, A. L.; Susha, A. S.; Caruso, F.; Sukhorukov, G. B.; Kornowski, A.; Kershaw, S.; Möhwald, H.; Eychmüller, A.; Weller, H. *Adv. Mater.* **2000**, *12*, 333.
(36) Rogach, A. L.; Kotov, N. A.; Koktysh, D. S.; Ostrander, J. W.; Ragoisha, G. A. *Chem. Mater.* **2000**, *12*, 2721.
(37) Radtchenko, I. L.; Sukhorukov, G. B.; Gaponik, N.; Kornowski, A.; Rogach, A. L.; Möhwald, H. *Adv. Mater.* **2001**, *13*, 1684.
(38) Susha, A. S.; Caruso, F.; Rogach, A. L.; Sukhorukov, G. B.; Kornowski, A.; Möhwald, H.; Giersig, M.; Eychmüller, A.; Weller, H. *Colloids Surf. A* **2000**, *163*, 39.
(39) Mamedova, N. N.; Kotov, N. A.; Rogach, A. L.; Studer, J. *Nano Lett.* **2001**, *1*, 281.
(40) Talapin, D. V.; Poznyak, S. K.; Gaponik, N. P.; Rogach, A. L.; Eychmüller, A. *Physica E* **2002**, *14*, 237.
(41) Demas, J. N.; Grosby, G. A. *J. Phys. Chem.* **1971**, *75*, 991.
(42) Kubin, R. F.; Fletcher, A. N. *J. Lumin.* **1982**, *27*, 455.
(43) Rogach, A. L. *Mater. Sci. Eng. B* **2000**, *69*, 435.
(44) Mamedov, A. A.; Belov, A.; Giersig, M.; Mamedova, N. N.; Kotov, N. A. *J. Am. Chem. Soc.* **2001**, *123*, 7738.
(45) Sun, J.; Gao, M.; Feldmann, J. *J. Nanosci. Nanotechnol.* **2001**, *1*, 133.
(46) Colvin, V. L.; Schlamp, M. C.; Alivisatos, A. P. *Nature* **1994**, *370*, 354.
(47) Glozman, A.; Lifshitz, E.; Hoppe, K.; Rogach, A. L.; Weller, H.; Eychmüller, A. *Isr. J. Chem.* **2001**, *41*, 39.
(48) Resch, U.; Weller, H.; Henglein, A. *Langmuir* **1989**, *5*, 1015.
(49) Gerion, D.; Pinaud, F.; Williams, S. C.; Parak, W. J.; Zanchet, D.; Weiss, S.; Alivisatos, A. P. *J. Phys. Chem. B* **2001**, *105*, 8861.
(50) Aldana, J.; Wang, A.; Peng, X. *J. Am. Chem. Soc.* **2001**, *123*, 8844.
(51) Gao, M.; Kirstein, S.; Möhwald, H.; Rogach, A. L.; Kornowski, A.; Eychmüller, A.; Weller, H. *J. Phys. Chem. B* **1998**, *102*, 8360.
(52) Peng, X.; Schlamp, M. C.; Kadavanich, A. V.; Alivisatos, A. P. *J. Am. Chem. Soc.* **1997**, *119*, 7019.
(53) Dabbousi, B. O.; Rodriguez-Viejo, J.; Mikulec, F. V.; Heine, J. R.; Mattoussi, H.; Ober, R.; Jensen, K. F.; Bawendi, M. G. *J. Phys. Chem. B* **1997**, *101*, 9463.
(54) Chemseddine, A.; Weller, H. *Ber. Bunsen-Ges. Phys. Chem.* **1993**, *97*, 636.
(55) Talapin, D. V.; Rogach, A. L.; Shevchenko, E. V.; Kornowski, A.; Haase, M.; Weller, H. *J. Am. Chem. Soc.* **2002**, *124*, 5782.
(56) Talapin, D. V.; Shevchenko, E. V.; Kornowski, A.; Gaponik, N.; Haase, M.; Rogach, A. L.; Weller, H. *Adv. Mater.* **2001**, *13*, 1868.
(57) Haubold, S.; Haase, M.; Kornowski, A.; Weller, H. *Chem. Phys. Chem.* **2001**, *2*, 331.
(58) Guzelian, A. A.; Banin, U.; Kadavanich, A. V.; Peng, X.; Alivisatos, A. P. *Appl. Phys. Lett.* **1996**, *69*, 1432.
(59) Bruchez, M. Private communication.
(60) Nethercot, A. H. *Phys. Rev. Lett.* **1974**, *33*, 1088.
(61) Schooss, D.; Mews, A.; Eychmüller, A.; Weller, H. *Phys. Rev. B* **1994**, *49*, 17072.